# Traveling waves in a water-immersed binary granular system vibrated within an annular cell

A. J. Smith,[1] M. C. Leaper,[2] Michael R. Swift,[1] and P. J. King[1]
[1]*School of Physics and Astronomy, University of Nottingham, Nottingham NG7 2RD, United Kingdom*
[2]*School of Chemical, Environmental and Mining Engineering, University of Nottingham, Nottingham NG7 2RD, United Kingdom*
(Received 10 January 2005; published 24 March 2005)

It has been known since the time of Faraday that vertically vibrated fine grains may spontaneously form piles through their interaction with a fluid. More recently, it has been observed that a fine binary mixture may separate under vertical vibration through the differential influence of the fluid on the two granular components. Here, we report a detailed study of a system of water-immersed bronze and glass grains held between two coaxial cylinders. Under vertical vibration, the bronze separates to form a layer above the glass, which itself breaks symmetry to form a pile. Symmetry is broken a second time by the bronze forming layers of different thicknesses upon the two slopes of the glass pile. The pile then travels as a wave with the thicker bronze layer upon its leading surface. We examine the conditions for these traveling waves and determine how their speed varies with particle size, frequency, and amplitude of vibration. A model is developed which provides a semiquantitative account of the wave motion.

DOI: 10.1103/PhysRevE.71.031303 PACS number(s): 45.70.−n, 81.05.Rm

## I. INTRODUCTION

Granular materials are known to exhibit a wide range of complex dynamical behaviors [1]. Here we describe a system in which purely vertical vibration leads to horizontal traveling waves. These waves are observed when a fluid-immersed binary granular mixture is vertically vibrated while being held between two coaxial cylinders. The waves rely for their existence on two phenomena which occur when fine grains interact under vibration with an interstitial fluid, Faraday piling, and the fluid-driven separation of binary mixtures.

Since the time of Chladni and Faraday it has been known that fine particulates may spontaneously form conical piles when placed upon a horizontal platform which is being vertically vibrated either by tapping or by continuous oscillation [2]. Within a vertically vibrated container, a body of grains may be observed to pile or tilt through the same "Faraday effect" [3–6].

Faraday's experiments suggested that these effects are associated with air movement induced by the throwing of the granular bed [2] and, despite some doubts, the involvement of the ambient fluid is now widely accepted [5–13]. Although the detailed mechanism and some important aspects of the behavior are still the subject of active debate [6,9–14], recent work in our own laboratory on water-immersed systems [15] broadly supports the proposal of Thomas and Squires [9,11], who suggested that the buildup of tilt is the result of horizontal fluid movement within the bed. Vibration of sufficient amplitude throws the bed of grains from the platform during each vibration cycle, the grains landing and settling later in the cycle. Early in bed flight the pressure below the bed is reduced as fluid is drawn down through it. If the upper surface of the bed is tilted, the horizontal component of this fluid flow accelerates grains horizontally, in a sense which enhances the tilt. Later in flight an overpressure develops below the bed as it approaches the platform, slowing the horizontal granular motion. The tilt builds up until it reaches an equilibrium. The construction of tilt due to horizontal fluid flow is then balanced during each cycle of vibration by grains cascading down the upper surface and by tilt destruction within the bed which occur when it lands [15].

The second feature upon which the traveling waves depend is the separation of a binary mixture that occurs under vertical vibration through its interaction with the ambient fluid [16,17]. As the bed is vibrated fluid is forced through the bed, downwards early in the vibration cycle, and upwards later in the cycle. If the fluid drag has a differential effect on the two components, they will tend to be drawn apart during the fluid movement. However, grains of the same type will tend to stay together since they are influenced similarly by fluid drag. Over many cycles of vibration the granular mixture will separate with the component having the larger value of $\rho d^2$ uppermost. Here $\rho$ is the granular density and $d$ is the particle diameter. The excellent separation which may be caused in this way depends upon "gaps" which open up between the separated beds during flight, ensuring local granular convection within each separated region, rather than global convection which would cause mixing [18].

In this paper we describe the behavior of a water-immersed system of spherical bronze and glass grains under vertical sinusoidal vibration when held between two coaxial cylinders. We observe that the grains separate with the bronze grains above the glass. The glass forms into a single Faraday pile with a bronze layer upon its slopes. Should the bronze not be of equal thickness on the two slopes of the glass pile, the pressure gradients which develop across the glass pile cause the glass and bronze to rotate together round the system, traveling as a wave. This movement maintains the inequality of the bronze thickness on the two slopes. We present a simple model for this behavior, based upon thrown granular beds within an incompressible fluid. This model explains the principal behaviors and gives a good semiquantitative account of the dependence of the rotational period upon the frequency and amplitude of vibration.

## II. EXPERIMENTAL TECHNIQUES

Bronze and glass grains were held between a pair of polymethylmethacrylate (PMMA) cylinders, positioned coaxially

 

using an upper and lower grooved Dural plate into which they were glued. The inner cylinder had an outer diameter of 30 mm, while the outer cylinder had an inner diameter of 52 mm. The cylinders were 46 mm high. The space between the cylinders could be filled through holes in the upper plate which could then be sealed with bungs. The axis of the cylinder assembly was held within ±0.2° of vertical and the assembly vibrated vertically in a manner which ensured accurate one-dimensional sinusoidal motion along this axis [17,18].

The vertical motion was monitored using a cantilever capacitance accelerometer system which displays the dimensionless ratio of the maximum acceleration to the acceleration due to gravity, $\Gamma = a\omega^2/g$ Here $a$ is the amplitude of vertical vibration of the cylinder assembly, $\omega = 2\pi f$ is the angular frequency, and $g$ is the acceleration due to gravity. The experiments have been performed using spherical bronze and soda-glass grains of densities $\rho_b = 8900\ \mathrm{kg\,m^{-3}}$ and $\rho_g = 2500\ \mathrm{kg\,m^{-3}}$, respectively. Each had a spread of grain diameters of about ±10% to avoid gross crystallization effects. The grains were inserted into the space between the cylinders through an upper hole and the filling completed with distilled water. The assembly was shaken to release any air bubbles and then refilled and sealed so that no visible air bubbles were contained within its volume.

The use of a fluid such as water offers a number of advantages for studying the effects of Faraday tilting and fluid-driven separation. First, considerably larger particles may be used, making the observation of granular motion far easier than for air. For nonturbulent fluid flow, the effects of fluid drag on the granular dynamics scale approximately as $\rho d^2/\eta$, where $\eta$ is the dynamic viscosity of the fluid [17,18]. At 20 °C, water is about 50 times more viscous than air, suggesting the use of particles ~7 times larger in diameter than for the observation of similar effects in air. The motion of these grains may readily be observed through the transparent cylinder walls using digital photography.

Second, the use of water eliminates the effects of static electricity which often slow and otherwise modify the dynamics of dry granular systems when they are shaken vigorously for long periods, particularly within an insulating box [17].

Third, within a liquid, the coefficient of restitution between grains is close to zero at low Stokes' numbers, lowering the granular temperature within the thrown beds, and maintaining a more constant bed porosity than would be the case for systems thrown in a gas such as air, where the coefficient of restitution is close to unity [15,19].

### III. OBSERVATION OF TRAVELING WAVES

The set of images of Fig. 1 shows the result of applying vibration at 50 Hz and $\Gamma = 4.0$ to an initially well mixed collection of bronze and glass grains, both species having diameters in the range 600–710 $\mu$m. The mixture consists of 25% bronze to 75% glass by volume. The mean granular bed depth is 12.7 mm. It may be seen that, under vibration, the grains separate into bronze-rich and glass-rich regions which become increasingly deficient in the minority component.

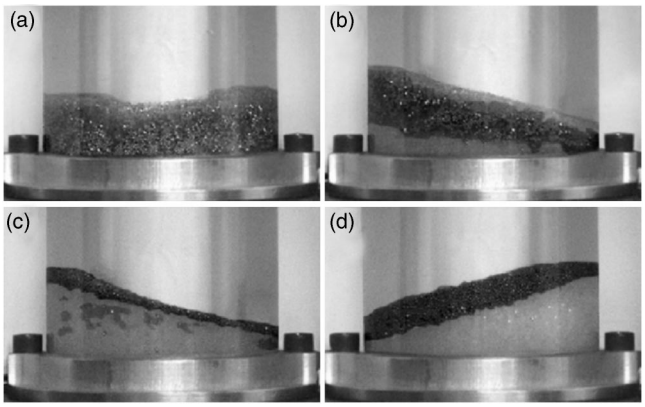


FIG. 1. The development of separation and piling following the application of vertical vibration of 50 Hz and $\Gamma = 4.0$ to a 25%:75% bronze glass mixture of 600–710 $\mu$m diameter spheres. The images are after times of (a) 0, (b) 7, (c) 41 and (d) 87 s.

Early in the motion, an almost pure bronze layer may form between an upper and a lower glass layer [Fig. 1(b)]. Soon, however, the bronze rises to the upper surface lying above a single glass region. As the separation proceeds, the lower glass region forms into a single pile.

Parts of the granular system then begin to move horizontally, the upper slope of the glass pile which has the most bronze forming the leading edge of a traveling wave. Soon, the granular system rotates as a whole about the vertical axis, the glass pile and the upper bronze layers moving as a wave without further changes in form. The images of Fig. 2 show almost one full rotation of the traveling wave about the axis of the system. It may be seen that the majority of the bronze grains lie on the leading edge of the wave, forming an approximately even layer, while a far thinner layer occurs on the trailing edge. An initially well-mixed system may rotate in either sense following separation and pile formation, but in all cases the rotation is such that the thicker bronze layer is on the leading edge of the wave. Within this coaxial geometry the granular behavior is essentially identical when viewed through the outer or inner cylinders once full separation has occurred; we do not then observe any appreciable radial component to the mean granular motion.

Figure 3 shows, schematically, the results of applying a range of frequencies and values of $\Gamma$ to the particle system shown in Figs. 1 and 2. In general the speed of granular motion increases rapidly with $\Gamma$, the line "$\alpha$" indicating the conditions for the completion of granular separation and piling on the time scale of 10 min. At low frequencies, within region B, the mixture separates almost completely with the bronze uppermost, lying above a glass pile. The bronze forms layers of the same mean thickness upon the two slopes of the glass pile. There are small temporal fluctuations in the horizontal position of the pile, but no mean direction of movement. At very low frequencies and high $\Gamma$, region A, separation occurs with the bronze above the glass, but no glass heap develops, probably as a result of the very high bed porosities which result from the large amplitudes of vibration found in this region.

Within region C traveling waves are observed. Throughout most of this region the separation is close to perfect, with

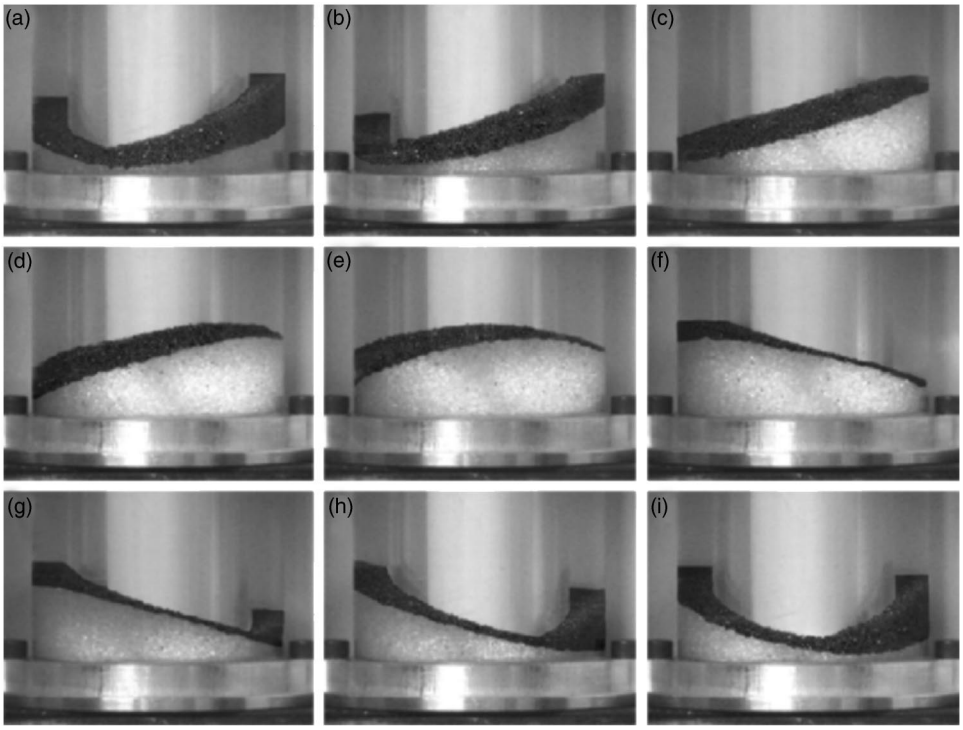


FIG. 2. The motion of the fully developed traveling wave configuration of a 25%:75% bronze glass mixture of 600–710 $\mu$m diameter spheres, under vertical vibration of 50 Hz and $\Gamma = 4.0$. The images (a)–(i) are in sequence and are spaced in time by about 2 s. Here the bronze and glass system is rotating clockwise as viewed from above, the granular motion being right to left as viewed.

pure bronze layers forming above a well-defined and almost pure glass heap; the bronze is thicker upon the leading edge of the glass pile. Only at lower values of $\Gamma$ and higher values of frequency within region C is the separation less than complete, with some bronze within the glass pile, and glass within the bronze. It is within region C, shown shaded, that we have carried out the following studies of traveling waves. Here, the the heap moves at a steady speed and the motion is therefore periodic. At higher frequencies, within region D, complex behavior is observed, with not only poor separation, but with the heap distorting and reforming as a function of time. Consequently, there is no well-defined period of oscillation in this region.

Within region C the bronze layers are of almost constant thickness over the larger parts of both the leading and training slopes of the traveling glass pile. Figure 4 shows, for $\Gamma = 4.0$, the thicknesses of the bronze layers measured half-way up the corresponding glass slope, plotted as a function of frequency. It is seen that the two thicknesses are very different at high frequencies, each being approximately independent of frequency. However, below 40 Hz, they approach one another and at lower frequencies become equal. At the same time the rate of rotation slows and the rotation ceases.

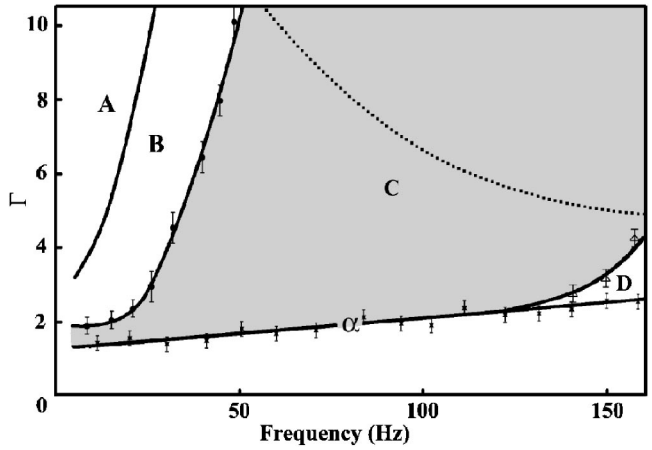


FIG. 3. Schematic $\Gamma$-$f$ diagram for a 25%:75% mixture of 600–710 $\mu$m bronze/glass particles, showing the regions of behavior described in the text. The dotted line shows the approximate boundary to the left of which the grains are thrown and settle within each cycle. The theory which we have presented is only valid within that part of region C which is to the left of this line. The error bars give an indication of our experimental uncertainty in estimating the positions of the various boundary lines.

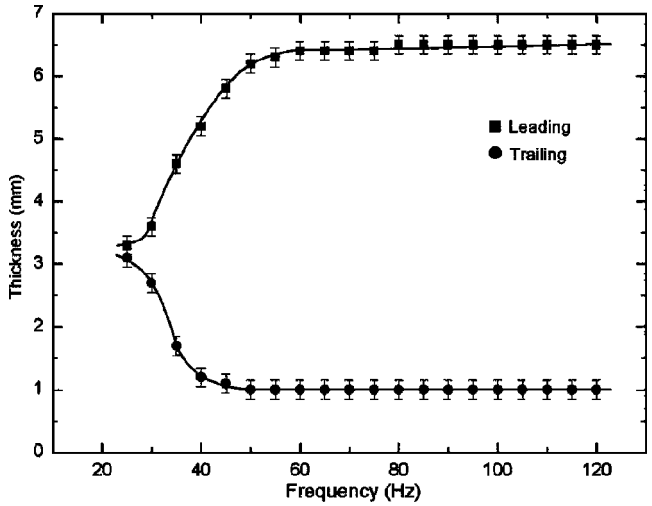


FIG. 4. The thicknesses of the bronze layers on the leading and trailing edges of the glass pile, plotted as a function of vibration frequency. The data are for $\Gamma = 4.0$.

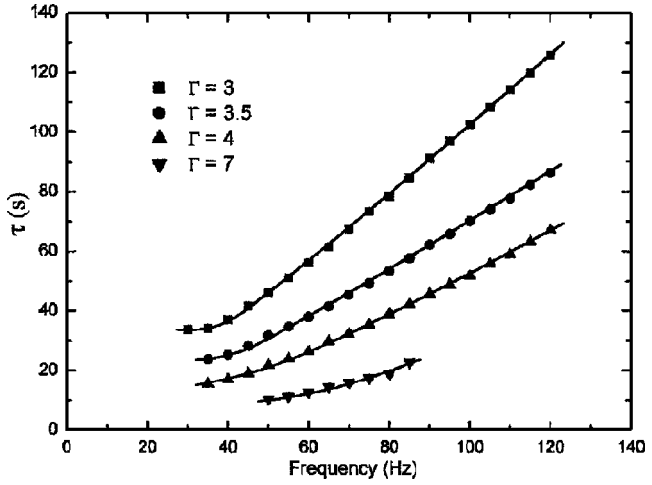


FIG. 5. The measured rotation period, $\tau$, vs frequency for four values of $\Gamma$. The points represent the experimental data, while the best fit lines are a guide to the eye.

The behavior then corresponds to region B of Fig. 3. It appears that the rotation is driven by differences in the thicknesses of the bronze layers. In Fig. 4 the sum of the thicknesses at high frequencies somewhat exceeds the sum of the thicknesses at low frequencies. This is possible due to the small but variable "reservoir" of bronze at the bottom of the slopes, a reservoir which travels with the wave.

Figure 5 shows the dependence of the observed period of rotation about the vertical axis, $\tau$, as a function of frequency, for four values of $\Gamma$. It is seen that, in each case, $\tau$ increases with frequency, slightly more rapidly than linear. As $\Gamma$ is increased the period rapidly reduces. This may be further seen from Fig. 6, which shows the dependence of $\log_{10}(\tau)$ upon $\log_{10}(\Gamma-1)$ for four different frequencies. $\Gamma$-1 rather than $\Gamma$ is used as the variable, since at $\Gamma=1$ no granular motion with respect to the container is expected. At low values of $\Gamma$-1, the data lie on straight lines over more than a decade of $\tau$, each having a gradient of $-2.1\pm0.1$, while at higher values of $\Gamma$-1 the gradient becomes less negative.

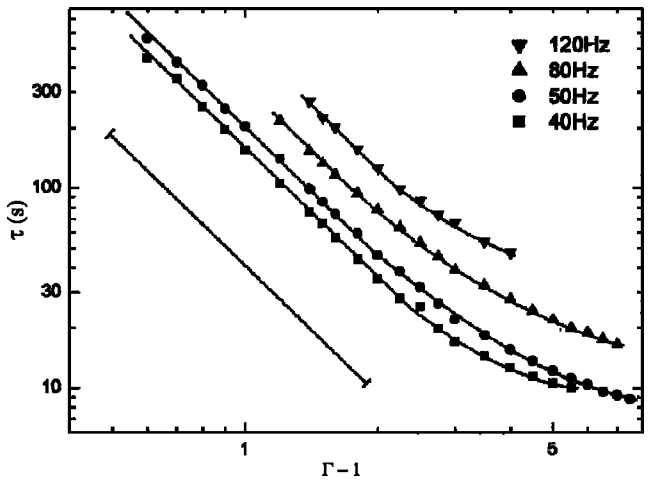


FIG. 6. Experimentally determined values of $\log_{10}(\tau)$ vs $\log_{10}(\Gamma\text{-}1)$ for four frequencies. The points represent the experimental data, while the best fit lines are a guide to the eye. The line to the left of the data has a slope of $-2.1$ and is also intended as a guide to the eye.

We have carried out further experiments in which we have used various sizes of grains, studying systems in which the bronze and glass grains are of equal or unequal sizes. Provided that the conditions for good separation are met, requiring $\rho d^2$ to be very different for the two species [18], traveling waves may be observed for particle sizes ranging from 250 to 1200 $\mu$m, usually over somewhat reduced ranges of frequency and $\Gamma$. However, the period of rotation has only a weak dependence upon particle size.

## IV. THEORY OF THE WAVE DYNAMICS

We will now present a model for the granular system which, despite the large number of simplifications and approximations, successfully explains many of the principal observations. The present experiments clearly show that the glass pile travels only in response to different thicknesses of bronze upon its two slopes. This suggests the following physical mechanism for the horizontal movement. Under vertical vibration the bronze is thrown higher than the glass since it has a higher density and is therefore less influenced by fluid damping. Gaps therefore develop between the bronze and glass beds. The pressure in the gaps will be less than ambient early in flight, as fluid is drawn down through the bronze beds, and greater than ambient later in flight as fluid is forced upwards. Unequal thicknesses of bronze on the two slopes will lead to different pressures under the two bronze beds, resulting in a net horizontal pressure across the glass pile. This pressure difference accelerates the glass bed early in flight and decelerates it later in flight, causing a net horizontal displacement during each cycle of vibration.

In deriving an expression for the period of rotation, first let us consider the vertical motion of a granular bed of thickness $h$, thrown from a horizontal platform moving vertically as $z_p = a\sin(\omega t)$. If the bed is considered to be a rigid porous plug moving in one dimension within a viscous fluid of finite density then it may be shown that the bed will take flight at a phase angle of $\sin^{-1}(1/\Gamma)$ and in flight will follow the equation [18,20,21]:

$$\left[1+\frac{\rho_f}{\rho}\frac{(1-\phi)}{\phi}\right]\dot{u}+\gamma u+\frac{(\rho-\rho_f)}{\rho}g=-\frac{(\rho-\rho_f)}{\rho}\ddot{z}_p, \quad (1)$$

where $u$ is the rate of change of the vertical position of the bed with respect to the container, $\phi$ is the porosity of the bed, $\rho_f$ is the fluid density, and $\gamma$ is a fluid damping parameter. If the fluid flow through the bed is laminar, then application of the linear term of the Ergun bed equation leads to [22]:

$$\gamma=\frac{150(1-\phi)\eta}{\rho\phi^3 d^2}. \quad (2)$$

It may also be shown [21] that, when the bed is in flight, the additional pressure just below the bottom of the bed due to its presence is given by [21]:

$$P=h(\rho-\rho_f)(1-\phi)(g+\ddot{z}_p+\dot{u}). \quad (3)$$

This pressure is in addition to the ambient pressure and to the pressure differences $\rho_f(g+\ddot{z}_p)\Delta z$ between any two points

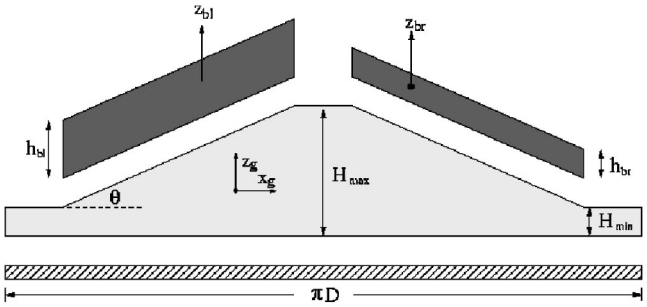


FIG. 7. Schematic diagram of the "unwrapped" glass pile and bronze layer configuration used in our model. The beds are in flight, having been thrown from the lower platform, shown hatched. The upper bronze layers are taken to be uniform in depth upon each slope, while the lower glass pile moves as a whole without changing shape. The symbols used are described in the text.

separated by a vertical distance $\Delta z$, due to the action of gravity and the accelerating frame on the mass of the liquid. It is to be noted that the equation of motion (1) does not contain the bed thickness, $h$, while the pressure, $P$, depends directly upon $h$. It is further to be noted that if the vertical motions of **two** distinct beds are considered then, while in flight and not in contact, the two beds are not aware of each other's presence within an incompressible fluid. A flight equation having the form of Eq. (1) will apply to each of them.

In order to predict the motion of our granular system and to estimate the period of rotation we apply these results to the motions of the bronze and glass beds. We consider grains held between two coaxial cylinders, the mean diameter being $D$. In systems in which the distance between the two cylinders is considerably less than $D$, negligible radial variation is observed in the mean granular motion; in the present model radial motion is taken to be zero. We therefore consider the simplified geometry shown in Fig. 7. The suffices $b$ and $g$ to refer to bronze and glass, respectively, and $r$ and $l$ to refer to the right and left hand sides of the diagram. The symmetric glass pile of slope angle $\theta$, has a maximum height $H_{\max}$ and a minimum height $H_{\min}$. A bronze layer of uniform depth $h_{bl}$ covers the left slope, while a bronze layer of depth $h_{br}$ covers the right slope. Each bed is considered as an object of uniform porosity $\phi_b$ or $\phi_g$. A bed may move in the $x$(horizontal) and $z$(vertical) direction during flight but we assume that it does not change either its shape or its orientation with respect to the horizontal.

Initially the lower platform, shown hatched in Fig. 7, begins to move vertically as $z_p = a\sin(\omega t)$. If $\Gamma = a\omega^2/g$ is greater than unity, the glass and bronze beds will be thrown from the platform. The bronze beds will fly higher and land later in time than the glass bed, due to the lower effect of fluid damping on the more dense bronze. It is supposed that $\Gamma$ is constrained so that both bronze and glass beds land and have time to settle before they are thrown again in the following vibration cycle. The dotted line shown in Fig. 3 gives a rough estimate of the upper limits of $\Gamma$ and frequency for which this is true.

We now suppose that the vertical motion of each bed is greater than the horizontal motion. This is generally true due to the low angle of the granular slopes; $\theta$ (Fig. 7) is typically in the range 10°–20°. As an approximation, we will use Eqs. (1)–(3) to calculate the vertical flight of the bronze and glass beds and the pressures under the bronze beds, and treat horizontal motions as a perturbation resulting from these pressures. In this approach the vertical motion of the bronze beds is then given by Eqs. (1) and (2) with appropriate values of the granular density, $\rho_b$, and porosity $\phi_b$. Note that, to this approximation, the two bronze beds undergo the same vertical flight. The pressure under the bronze beds will vary during their flight and since the two beds are of different thickness there will be, at any particular height $z$, a net pressure difference between the left and right hand sides of the glass bed, given by Eq. (3) as

$$\Delta P = (h_{bl} - h_{br})(\rho_b - \rho_f)(1 - \phi_b)(g + \ddot{z}_p + \dot{u}_b). \tag{4}$$

The glass bed may move horizontally in response to this pressure difference while it is in flight. The vertical motion of the glass bed may be obtained using Eq. (1) again with appropriate values of the granular density, $\rho_g$, and porosity, $\phi_g$. We note that, since Eq. (1) indicates that vertical flight is independent of the bed depth, it is to be expected that all parts of the glass bed undergo the same vertical motion. In experiments, the bed is observed to maintain its shape while undergoing slow internal convection. In the current model we assume that the glass bed moves as a rigid porous body. The horizontal pressure gradient across the glass bed will cause motion both of the glass grains and the fluid contained within the glass bed. At the frequencies used here we may assume that they move together. The equation of motion for the horizontal motion of the glass bed is then given by

$$M\ddot{x}_g = s(H_{\max} - H_{\min})\Delta P, \tag{5}$$

where $s$ is the radial distance between the two concentric cylinders and $M$ is the effective mass of the glass bed, given by

$$M = \frac{s\pi D}{2}(H_{\min} + H_{\max})[\rho_g(1 - \phi_g) + \rho_f\phi_g]. \tag{6}$$

The net horizontal motion of the glass bed, $\delta x_g$, may be obtained by integrating $\ddot{x}_g$ twice with respect to time, from the time of take-off to the time of landing of the glass bed. $\delta x_g$ is the motion per cycle of vibration and is related to the period of rotation of the system about its vertical axis, $\tau$, by $\tau = \pi D/(f\delta x_g)$. Thus $\tau$ is given by

$$\tau = \frac{\pi^3 D^2}{(h_{bl} - h_{br})}\frac{(H_{\max} + H_{\min})}{(H_{\max} - H_{\min})}\frac{[\rho_g(1 - \phi_g) + \rho_f\phi_g]}{(\rho_b - \rho_f)(1 - \phi_b)\omega I(\Gamma, \omega)}, \tag{7}$$

where $I(\Gamma, \omega)$ is the double integral of $g + \ddot{z}_p + \dot{u}_b$ taken over the flight time of the *glass* bed.

We note that each bronze bed is drawn into the region of reduced pressure which exists below it early in flight, acquiring horizontal motion which tends to move it in an upslope direction. Later in flight these horizontal motions are brought to a halt by the overpressures below the bronze beds. The net motion drives the bronze beds uphill, as we observe. Experi-

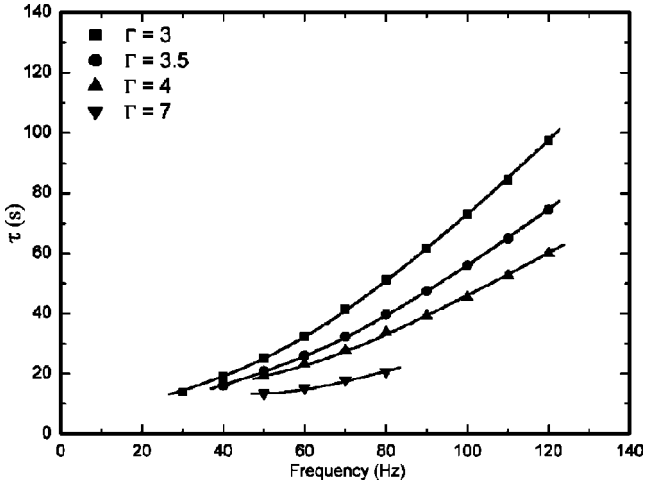


FIG. 8. The rotation period, $\tau$, determined from theory, vs frequency, for four values of $\Gamma$. The points represent estimations from the theory using the experimentally determined parameters described in the text. The best fit lines are a guide to the eye.

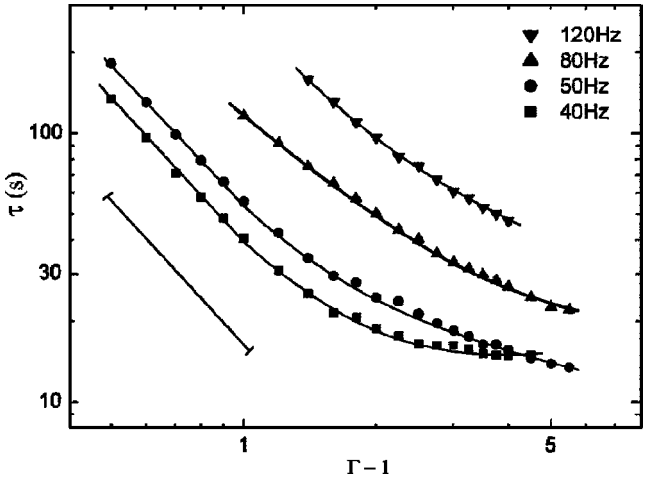


FIG. 9. $\log_{10}(\tau)$ determined from theory, vs $\log_{10}(\Gamma\text{-}1)$, for four values of frequency. The points represent estimations from the theory using the experimentally determined parameters described in the text. The best fit lines are a guide to the eye. The line to the left of the data has a slope of −1.49 and is also intended as a guide to the eye.

mentally, the net motion within the bronze beds is upslope, compensated by downslope granular motion at the upper surfaces.

## V. COMPARISON BETWEEN THEORY AND EXPERIMENT

We have compared our experimental measurements of $\tau$ with numerical predictions using the method outlined earlier. We take the mean porosity of the heavily damped glass bed as $\phi_g = 0.42$, the experimentally measured porosity for the loose random packing of spheres of our range of sizes; the bronze beds are more kinetically active under vibration and we assume the slightly higher value of $\phi_b = 0.44$ for the mean in-flight porosity of these beds. These values were chosen to represent typical porosities under these vibratory conditions. Variations in porosity of the glass bed have little effect on the time period. However, changes in the porosity of the bronze bed have a much larger influence on the period through Eqs. (1) and (2). An increase in $\phi_b$ of 0.02 increases the time period by of order 10%.

The theory given earlier has been used to predict the dependence of the period upon frequency and $\Gamma$. We use as inputs to our predictions a number of experimentally determined parameters, namely $H_{\max}$, $H_{\min}$, $h_{bl}$ and $h_{br}$, which have been measured as a function of the two principal parameters $\omega$ and $\Gamma$. The mean diameter of the granular annulus, $D$, is 41 mm, while the diameter of both the bronze and the glass grains, is taken to be $d = 655$ $\mu$m, the mean value used in the experiments. For each frequency and $\Gamma$ we have obtained the vertical motion of the bronze and glass beds through Eqs. (1) and (2) and then carried out the double integration to obtain $\tau$.

Figure 8 shows the predicted values of the period as a function of frequency for the four values of $\Gamma$ used in making the measurements of Fig. 5. The two sets of graphs are seen to have very similar form. In Fig. 8 the period rises somewhat more rapidly than linearly with frequency and as $\Gamma$ is increased the period falls rapidly. However, while the general form of the measured and predicted data is very similar, the predicted periods span a somewhat more limited range of time than do the experimental data.

Figure 9 shows the predicted values of the period, plotted against $\Gamma$-1 using logarithmic scales, and for the four different frequencies used in the measurements of Fig. 6. Again the general form of the two sets of data is very similar, the predicted period falling as $\Gamma$ is increased, following a straight line on the log-log plots for low $\Gamma$ but decreasing more slowly for higher values of $\Gamma$. Here, however, the slope is $-1.5 \pm 0.1$. While the measured and predicted values are similar at high values of $\Gamma$, the agreement becomes progressively worse as $\Gamma$ is reduced, reflecting the differences in gradient. It is to be noted that both in the measurements and in the predictions the data for 40 and 50 Hz tend to cross at higher values of $\Gamma$. This is due to the tendency for the bronze thicknesses, $h_{bl}$ and $h_{br}$, to equalize at lower frequencies and higher values of $\Gamma$, causing the period to increase.

Finally, we note that the model predicts only a weak dependence of the period, $\tau$, on the grain size, $d$. The glass grain size does not enter Eq. (7). Decreasing the bronze grain size increases the fluid damping of the bronze beds, reducing the height to which they are thrown. The net effect on $I(\Gamma, \omega)$, through which $d_b$ enters the expression for $\tau$, is very small. The effect of nonlinear bed resistance to flow is also a weak influence for similar reasons. Inclusion of the nonlinear term of the Ergun bed equation reduces the predicted values of $\tau$ by less than 10%.

## VI. DISCUSSION

We have studied a phenomenon which depends upon two of the major features found in the behavior of vertically vibrated fluid-immersed grains, Faraday tilting, and granular separation. Together, these effects are responsible for the unusual behavior of a binary granular system, in which a wave

rotates about a vertical axis under the application of purely vertical vibration.

This behavior may be explained by considering the motion of the beds as they are thrown by the vibration within an incompressible fluid. In the presence of the fluid the glass grains form a Faraday pile, covered by a bronze layer. The reduced pressure under the bronze beds early in flight causes up-slope movement which, compensated by down-slope surface movement, causes the bronze grains to form almost uniform layers upon the slopes of the glass pile. If, for any reason, the thicknesses of bronze upon the two glass slopes become unequal, then the different pressures below the bronze layers will cause the glass pile to move horizontally, taking the bronze layers with it. The difference in thickness between the two bronze layers is maintained by the movement of the pile with respect to the small reservoir of bronze at the bottom of the slopes, movement which encourages more bronze to be taken up into the bronze layer which is already thicker.

Unusually for a granular system, this configuration offers the opportunity to predict the period of rotation using an analytical model, rather than having to resort to methods such as particle based simulation. Our model treats the bronze and glass beds as rigid porous plugs for which the vertical motion dominates, horizontal motions being considered as a perturbation. Such a model has a number of weaknesses. In a more detailed treatment, coupled equations for the vertical and horizontal motions would no doubt be considered. While the convective motion within the more compact glass bed is slow, and it is a good approximation to consider it as a rigid porous plug, the bronze layers exhibit appreciable internal granular motion, both upslope within each bed and downslope at the upper surfaces.

Despite these weaknesses, the model is successful in capturing the essential features of the problem and in providing semiquantitative estimates of the rotational period, $\tau$, which have many features in common with the experimentally determined values. The glass pile is predicted and observed to move with the thicker bronze layer upon its leading edge. The dependence of the period upon frequency is both predicted and observed to be slightly more rapid than linear in each case, and to decrease in gradient with increasing $\Gamma$. The period is shown to vary as $\tau \sim 1/(\Gamma\text{-}1)^{\xi}$ at lower values of $\Gamma$, both experimentally and in our model predictions, the experimental value of $\xi$ being $-2.1 \pm 0.1$ while the model offers $\xi = -1.5 \pm 0.1$. While the experimental values for the period are close to the predicted values at higher $\Gamma$, the agreement becomes progressively worse as $\Gamma$ is lowered. This suggests the influence of what is probably the most important omission from our model, friction with the walls of the container. However, while the effect of friction is expected to become more important at lower values of $\Gamma$, it is not at present well characterized. We have not, therefore, attempted to incorporate it into our model, which has been principally used to understand the physical mechanisms behind the observed wave motion.

Finally, we note that related effects may be observed if an immersed granular mixture, of the type which we have described, is contained inside a single vertical cylinder. Under vertical vibration the mixture separates with the bronze uppermost and the granular system tilts. Over ranges of frequencies and $\Gamma$ the bronze is distributed nonuniformly across the surface of the tilted glass bed. The tilted granular system then rotates about the vertical axis. However, the granular motion contains radial components, and the extent to which a theory similar to the one presented here may be applied is under investigation.

## ACKNOWLEDGMENTS

We are grateful to the Engineering and Physical Sciences Research Council for financial support and for the loan of a high speed digital camera, to Makin Metal Powders Ltd. for their gift of powders, and to the workshop staff of the School of Physics and Astronomy for their skills and enthusiasm.

[1] H. M. Jaeger, S. R. Nagel, and R. P. Behringer, Rev. Mod. Phys. **68**, 1259 (1996).
[2] M. Faraday, Philos. Trans. R. Soc. London **52**, 299 (1831).
[3] B. Thomas, Y. A. Liu, R. Chan, and A. M. Squires, Powder Technol. **52**, 77 (1987).
[4] P. Evesque and J. Rajchenbach, Phys. Rev. Lett. **62**, 44 (1989).
[5] C. Laroche, S. Douady, and S. Fauve, J. Phys. (Paris) **50**, 699 (1989).
[6] H. K. Pak, E. van Doorn, and R. P. Behringer, Phys. Rev. Lett. **74**, 4643 (1995).
[7] E. Clement, J. Duran, and J. Rajchenbach, Phys. Rev. Lett. **69**, 1189 (1992).
[8] P. Evesque, J. Phys. (Paris) **51**, 697 (1990).
[9] B. Thomas and A. M. Squires, Phys. Rev. Lett. **81**, 574 (1998).
[10] K. Kumar, E. Falcon, K. M. S. Bajaj, and S. Fauve, Physica A **270**, 97 (1999).
[11] B. Thomas, M. O. Mason, and A. M. Squires, Powder Technol. **111**, 34 (2000).
[12] J. Duran, Phys. Rev. Lett. **84**, 5126 (2000).
[13] J. Duran, Phys. Rev. Lett. **87**, 254301 (2001).
[14] R. P. Behringer, E. van Doorn, R. R. Hartley, and H. K. Pak, Granular Matter **4**, 9 (2002).
[15] R. J. Milburn, M. A. Naylor, A. J. Smith, M. C. Leaper, K. Good, M. R. Swift, and P. J. King Phys. Rev. E **71**, 011308 (2005).
[16] N. Burtally, P. J. King, and M. R. Swift, Science **295**, 1877 (2002).
[17] N. Burtally, P. J. King, M. R. Swift, and M. C. Leaper, Granular Matter **5**, 57 (2003).
[18] M. C. Leaper, A. J. Smith, M. R. Swift, P. J. King, H. E. Webster, N. Miles, and S. Kingman, Granular Matter (to be published).
[19] P. Gondret, M. Lance, and L. Petit, Phys. Fluids **14**, 643 (2002).
[20] W. von Kroll, Forsch. Geb. Ingenieurwes. **50**, 2 (1954).
[21] R. Jackson, *The Dynamics of Fluidized Particles*, (Cambridge University Press, Cambridge, UK, 2000), Chap. 2.
[22] S. Ergun, Chem. Eng. Prog. **48**, 89 (1952).